Mycobacterial infection of macrophages results in membrane-permeable phagosomes

R. Teitelbaum*, M. Cammer†, M. L. Maitland*, N. E. Freitag‡, J. Condeelis§, and B. R. Bloom¶‖

*Department of Immunology and Microbiology, Wayne State University School of Medicine, Detroit, MI 48201; ‡Department of Microbiology and Immunology, §Department of Anatomy, and †Analytical Imaging Facility, Albert Einstein College of Medicine, New York, NY 10461; and *Harvard School of Public Health, Boston, MA 02115

Contributed by Barry R. Bloom, September 7, 1999

Cell-mediated immunity is critical for host resistance to tuberculosis. T lymphocytes recognizing antigens presented by the major histocompatibility complex (MHC) class I and class II molecules have been found to be necessary for control of mycobacterial infection. Mice genetically deficient in the generation of MHC class I and class Ia responses are susceptible to mycobacterial infection. Although soluble protein antigens are generally presented by macrophages to T cells through MHC class II molecules, macrophages infected with *Mycobacterium tuberculosis* or bacille Calmette-Guerin have been shown to facilitate presentation of ovalbumin through the MHC class I presentation pathway via a TAP-dependent mechanism. How mycobacteria, thought to reside within membrane-bound vacuoles, facilitate communication with the cytoplasm and enable MHC class I presentation presents a paradox. By using confocal microscopy to study the localization of fluorescent-tagged dextrans of varying size microinjected intracytoplasmically into macrophages infected with bacille Calmette-Guerin expressing the green fluorescent protein, molecules as large as 70 kilodaltons were shown to gain access to the mycobacterial phagosome. Possible biological consequences of the permeabilization of vacuolar membranes by mycobacteria would be pathogen access to host cell nutrients within the cytoplasm, perhaps contributing to bacterial pathogenesis, and access of microbial antigens to the MHC class I presentation pathway, contributing to host protective immune responses.

Cell-mediated immunity plays a major role in host defense against mycobacterial infections. Presentation of mycobacterial antigens by both the MHC class I and class II families is critical to protection because adoptive transfer of the T cells restricted by these molecules enhances survival (1). Additionally, mice genetically deficient in β_2-microglobulin, resulting in a lack of MHC class I and class I-like molecule expression (2), and mice depleted of CD8 T cells (1) more readily succumb to infection with *Mycobacterium tuberculosis* (*M. tb*).

Soluble antigens and phagocytosed bacteria, including mycobacteria, ultimately localize within membrane-bound endocytic vesicles (3, 4), where antigens are processed for association with MHC class II molecules and presented to $CD4^+$ T cells (5). Peptides presented through the MHC class I pathway generally derive from within the cytoplasm, where they are transported to the lumen of the endoplasmic reticulum by the transporter protein, TAP, for association with MHC class I molecules (5). Because mycobacteria remain within a vacuolar compartment, the mechanism of presentation of mycobacterial antigens through MHC class I molecules is highly problematic. Previously, it has been shown that infection of macrophages with bacille Calmette-Guerin (BCG) or *M. tb* facilitated presentation of soluble antigens (6), by a pathway that is TAP-dependent. Thus, mycobacterial infection facilitated peptide access to the cytoplasm for presentation on MHC class I, despite its presumed intracellular localization within membrane-bound vacuoles.

The current studies were undertaken to establish whether vacuoles containing mycobacteria become permeable to macromolecules located in the cytosol. Using confocal microscopy, we assessed colocalization of fluorescent signals from labeled mycobacteria within infected macrophages microinjected intracytoplasmically with tagged molecules of varying sizes. Our results indicate that viable mycobacteria have the ability to facilitate transit of macromolecules between the cytosolic and vacuolar compartments of infected cells, which has implications for both pathogenicity and immunity.

Materials and Methods

Cell Lines. The C57BL/6-derived murine bone marrow macrophage cell line BMA3.1A7 (7) was a kind gift from Kenneth Rock (University of Masachusetts Medical School). Cells were maintained as described (6).

Construction of pYUB 921. The FACS-optimized mutant 2 of the green fluorescent protein (GFP) gene from *Aqueorea victoria* (8) was kindly provided by S. Falcow (Stanford University). GFP was amplified by the PCR with primers: 5′-TTGCGGATCCAAGTAAAGGAGAAGAACTTTTCA CT-3′ and 5′-CGGAATTCCTATTTGTATAGTTCATCCATCCATGCCATG-3′. The reaction product was digested with *Bam*HI and *Eco*RI and was cloned into the appropriate sites within the mycobacteria/*E. coli* shuttle vector PMV-261 (9).

Preparation of Mycobacterial Strains. BCG (Connaught Laboratories) was transformed with pYUB 921 at room temperature as described (10). Transformants, designated "BCG-GFP" were plated on Middlebrook 7H10 agar (Difco) supplemented with glycerol (Sigma), 0.05% Tween-80 (Sigma), 10% OADC enrichment media (BBL), and kanamycin (Sigma) at a concentration of 50 μg/ml for plasmid selection. Plates were kept at 37°C for 21 days. A single colony was inoculated into 50 ml 7H9 (Difco), was supplemented as above, and was incubated in roller bottle culture at 37°C to mid-log phase. Bacteria were washed in PBS and were frozen in 10% glycerol/PBS in 1-ml aliquots at −70°C. Representative vials were thawed, serially diluted, and plated on 7H10 to determine the number of viable bacilli by colony forming units. Expression of the protein was verified by fluorescence microscopy and flow cytometry. Green fluorescent *Mycobacterium smegmatis*, designated "SMEG-GFP," were generated by transformation of strain mc^2155 as described (11). Frozen stock vials of SMEG-GFP were prepared similar to BCG-GFP.

Construction of *Listeria monocytogenes* Strains Expressing GFP. *L. monocytogenes* strain 10403S (serotype 1/2b) is resistant to streptomycin and has an LD50 for mice of 2×10^4 (12). DP-L2161, a 10403S derivative containing a chromosomal deletion of hly, has been described (13). *L. monocytogenes* strains were stored at −70°C in brain–heart infusion broth (Difco) containing 20% glycerol.

Abbreviations: BCG, bacille Calmette-Guerin; *M. tb*, *Mycobacterium tuberculosis*, GFP, green fluorescent protein; moi, multiplicity of infection; LLO, listeriolysin O.

‖To whom reprint requests should be addressed at: Office of the Dean, Harvard School of Public Health, 677 Huntington Avenue, Boston, MA 02115. E-mail: barry_bloom@harvard.edu.

The publication costs of this article were defrayed in part by page charge payment. This article must therefore be hereby marked "*advertisement*" in accordance with 18 U.S.C. §1734 solely to indicate this fact.

Escherichia coli HB101 was used as the host strain for recombinant plasmids. Plasmid pSPAC, a shuttle vector containing the isopropyl β-D-thiogalactoside-inducible Pspac promoter (14), was a kind gift of David Dubnau (New York Public Health Research Institute). Plasmid pGFPuv was from CLONTECH.

Primers GFP-1 (5′GCT-CTA-GA*A-GGA-GGA*-AAA-ATA-TGA-GTA-AAG-GAG-AAG-AAC-3′) and GFP-2A (5′-AAC-TGC-AGC-TAT-TTG-TAT-AGT-TCA-TCC-3′) were designed to amplify gfp coding sequences from plasmid pGFPuv using the PCR and to introduce a Gram-positive ribosome binding site derived from SD1 of ermC (15) (italicized sequence of GFP-1) upstream of gfp. The PCR amplified product was digested with *Xba*I and *Pst*I and was subcloned into pSPAC to yield pNF518. Plasmid pNF518 was introduced into *L. monocytogenes* strains 10403S and DP-L2161 (13) by electroporation (16). Transformants were isolated by growth at 37°C on BHI agar containing 1 mM isopropyl β-D-thiogalactoside and 10 g/ml chloramphenicol to generate NF-L543 [10403S = pNF518, or listeriolysin O (LLO) + GFP] and NF-L519 (DP-L2161 = pNF518, or LLO − GFP). Before infection of BMA3.1A7 cells, single colonies of NF-L5433 and NF-L519 were used to inoculate BHI broth containing 1 mM isopropyl β-D-thiogalactoside and 10 g/ml chloramphenicol, and cultures were grown overnight at 37°C. Overnight cultures were backdiluted to obtain an optical density of 0.8, were washed once, and were resuspended in DME-C containing isopropyl β-D-thiogalactoside.

***In Vitro* Infection with Live Mycobacteria.** BMA3.1A7 cells were plated at a concentration of 5×10^4 cells in 200 μl, on 35-mm Petri dishes containing number 1.5 glass coverslip bottoms (Mat-tek, Ashland, MA). Macrophage infection was carried out 4 hours after initial plating. BCG-GFP frozen stocks were thawed and grown in 7H9 supplemented media for no longer than 12 hours before macrophage infection, facilitating sufficient GFP expression without changing the CFU. BCG-SMEG was similarly incubated for 3 hours before macrophage infection, and the concentration was confirmed by measuring OD. Cultures were washed and resuspended in DME-C media, were sonicated, and were added to the macrophages in a total volume of 200 μl, at a multiplicity of infection (moi) of 6:1, mycobacteria to macrophages. BCG-GFP devoid of clumps were obtained as follows: postsonication, bacilli were passed through a 5-μm pore size filter (Micron Separations, Westboro, MA) and were added to the macrophages, at an moi of ≈2:1. The moi was determined spectrophotometrically, where an optical density of 1.0 was determined to contain 10^8 bacilli per milliliter. Macrophage infection was carried out for a period of 18–36 hours. After infection, cells were carefully washed twice with prewarmed fresh DME-C. For some studies, the BCG-GFP were killed by fixing in 10% neutral buffered formalin for 30 minutes.

Macrophages plated as above were also infected with *L. monocytogenes* expressing GFP. Ten hours after initial macrophage seeding, LLO^+ strains of *L. monocytogenes* expressing GFP (LLO + GFP) were added at an initial moi of ≈10:1 and were incubated at 37°C for 1 hour, at which time cells were washed twice, as described above. LLO^- strains of *L. monocytogenes* expressing GFP (LLO^- + GFP) were added at an moi of ≈10:1, as determined spectroscopically, and were incubated with macrophages for 4 hours, at which time cells were washed as above.

Fluorophores. Texas Red-tagged dextrans (3, 40, 70, and 2,000 kDa), Texas Red-tagged ovalbumin, and Oregon Green-tagged polystyrene beads, 0.5 μm (FluoSpheres), were purchased from Molecular Probes. Uncoupled fluorochrome was removed from each sample by centrifugation through a G50 Sephadex microspin column (Amersham Pharmacia). Sterilization was achieved by filtration of the coupled dye through a 0.45-μm pore size microfilter (Millipore).

Macrophage Microinjection. Infected BMA3.1A7 cells were injected with the tagged molecules listed above, with the aid of a Micromanipulator 5171 and a Transjector 5426 plus (Eppendorf). Needles were pulled on a Sutter pipette puller, model P87, and were backfilled with 4-μl samples by using microloaders (Eppendorf). Macrophages were microinjected with an initial pressure of 600 kPa.

Confocal Laser Microscopy. To facilitate immediate visualization of the microinjected dyes, the microinjection apparatus was mounted directly on the Nikon Diaphot with 60× n.a. 1.4 Planapo optics for use with the Bio-Rad MRC 600 confocal fluorescence microscope, equipped with a Krypton/Argon laser. The pinhole aperture was closed at 4 mm or smaller, and the absence of any emission "bleed-through" from the green channel into the red channel was ascertained before any data collection. Serial optical sections were collected in incremental steps at 0.9 μm for each sample analyzed. The z series collection was initiated once diffusion of the injected marker was determined by imaging fluorescence. Diffusion occurred across the cell in typically <1 minute after microinjection. Injected cells were imaged as soon as possible after microinjection, as well as ≈10 minutes after initial data collection, and were compared to verify their condition after the injection.

Optical theory and measurements obtained by using the reflection mode of the confocal microscope suggest a limit of resolution along the *z* axis of ≈0.8 μm (17). In practice, using fluorescent-tagged beads, we have found the resolution along the *z* axis to be comparable to that obtainable along the *x* and *y* axes. Oregon green-tagged polystyrene beads were suspended in 3-kDa Texas Red-tagged dextrans, were placed on poly-L-lysine coated slides, were covered with a number 1.5 coverslip, were sealed with nailpolish, and were viewed with the same settings as described above. Beads that were ≤0.5 μm were readily resolved as excluding the red tagged dextrans, when successive optical sections were viewed, indicating the resolution in the *z* axis was ≈0.5 μm.

Quantitation. Raw images from the Bio-Rad MRC 600 were imported into the software package NIH-IMAGE. Images were montaged, were imported into ADOBE PHOTOSHOP (Adobe Systems, Mountain View, CA), and were merged as RGB color. Colocalization of the two fluorescent signals was taken as a measure of macromolecule accessibility to the BCG-GFP compartment. Colocalization was scored on the merged images by two rigorous criteria: (*i*) colocalization revealed bacilli that appeared yellow through every plane of the z series of each bacterium; and (*ii*) examination of the intracellular area of signal colocalization in the red channel only revealed that no region within the phagosome was impenetrable to the tagged injected macromolecules. Bacilli yielding only one or neither of the two criteria were scored as "not colocalized." Thus, yellow bacilli found within regions impenetrable to the injected tagged-macromolecules in some, but not all, of the optical sections containing each bacterium within the series were scored conservatively as failing to demonstrate signal colocalization. At least 15 infected cells and more than 50 bacilli were enumerated for each data group. Data are pools of at least three independent experiments.

Results

BCG Infection of Macrophages Facilitates Phagosomal Permeability to Cytoplasmic Macromolecular Markers. To ascertain whether macrophage phagosomes containing mycobacteria were permeable to cytoplasmic markers in a live cell system, biohazard considerations necessitated the development of an *in vitro* culture system using BCG. Previously, BCG was shown to facilitate presentation of ovalbumin to T cells in an MHC class I-restricted fashion, although less efficiently than virulent *M. tuberculosis* (6). Soluble dextrans coupled to the Texas Red fluorochrome were microinjected into the cytoplasm of macrophages previously infected with BCG ex-

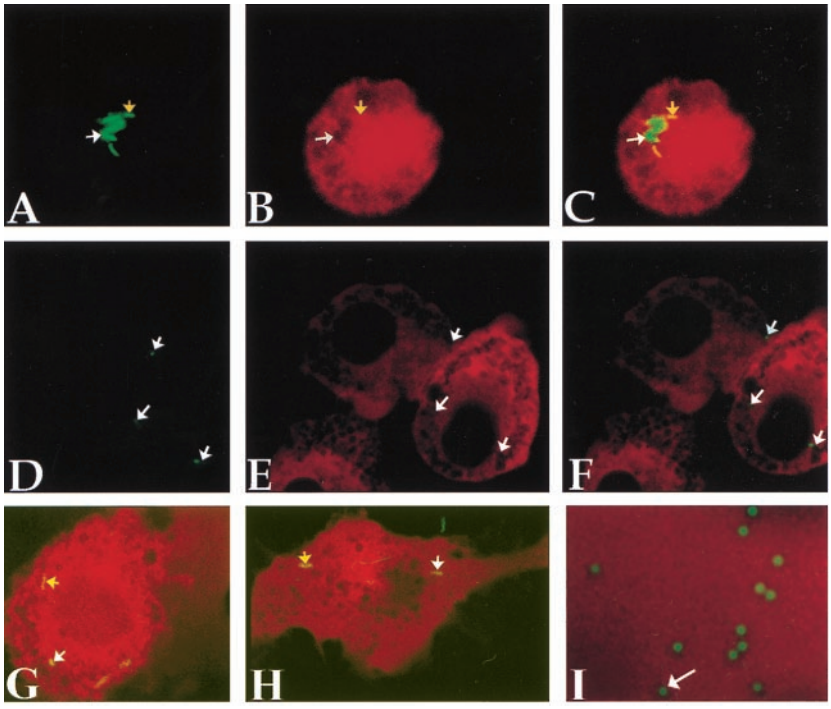

Fig. 1. Mycobacteria reside within permeable phagosomes admitting molecules up to 70 kDa. Macrophages infected with GFP-BCG for 18 hours were microinjected with Texas Red-tagged dextrans (3 kDa) and immediately were visualized by confocal microscopy. *A* and *D* show fluorescence in the green channel only, *B* and *E* show fluorescence in the red channel only, and *C*, *F*, *G*, and *H* are merged images. Colocalization of green fluorescent bacilli (*A*, yellow arrow) with 3-kDa-sized Texas Red-tagged dextrans (*B*, yellow arrow) manifested as yellow bacilli upon merging of the two channels (*C*, yellow arrow). Not all GFP-BCG (*A*, white arrow) are found within membrane-permeable vesicles (B, white arrow), and therefore did not exhibit signal colocalization (*C*, white arrow). Microinjection of 2,000-kDa-sized dextrans revealed green bacilli (*D*, white arrow) within vesicles clearly impermeable to the infected dextrans (*E* and *F*, white arrows). Mycobacterial phagosomes are permeable to injected proteins, within the appropriate size range, as ovalbumin accesses the mycobacterial phagosome (*G*, yellow arrow). Molecules of up to 70 kDa in size access the mycobacterial phagosome, as evidenced by the presence of yellow bacilli indicating signal colocalization (*H*, yellow arrow). Colocalization is not a limit of resolution artefact as Oregon-green-tagged beads ≤ 0.5 μm are readily resolved from the surrounding Texas-red-tagged dextrans (*I*, white arrow).

pressing GFP. Access of the dextrans to the mycobacterial phagosome, a direct measure of vacuolar membrane permeability, was established by determination of the extent of colocalization of the two signals by confocal microscopy. Tagged dextrans 3-kDa in size were able to gain access to phagosomes containing live BCG (Fig. 1 *A–C*). Bacilli were seen clearly to occupy a region (Fig. 1*A*) completely accessible to the dextrans (Fig. 1*B*), as evidenced by the intensity of fluorescence in the red channel, at these coordinates. Not all phagosomes, however, were accessed by the dextrans. Lack of colocalization of the two signals was detected by the presence of a green bacillus (Fig. 1*A*) within a circumscribed region with minimal fluorescence in the red channel (Fig. 1*B*), denoting an impermeable vacuole containing the bacillus. For each bacillus examined, a sequential optical series (z series) was recorded to determine signal colocalization at every plane of section. Lack of signal colocalization at any single plane of section, even with a majority of planes revealing colocalization, was scored conservatively as bacilli within impenetrable vesicles. Some mycobacterial phagosomes were similarly permeable to larger macromolecules 40 kDa (data not shown) in size. Colocalization of the two signals was not the result of a peculiarity of tagged dextrans used as intracellular markers, as Texas Red-tagged ovalbumin (45 kDa) microinjected into BCG-GFP-infected macrophages revealed a similar phenomenon (Fig. 1*G*). Microinjection of molecules as large as 70 kDa accessed the mycobacterial phagosome (Fig. 1*H*). Microinjection of 2,000-kDa-sized dextrans, however, failed to reveal signal colocalization at any plane of section (Fig. 1 *D–F*); thus, mycobacterial vesicles revealed a size-restricted access to the cytoplasm.

Fluorescent Signals from the Microinjected Dextran and Mycobacteria Colocalized at Every Plane of Optical Section. Successive optical sections were collected in a z series and were analyzed for each of the nine data groups examined. A representative series is shown in Fig. 2. BCG phagosomal membrane permeability revealed colocalization of the 40-kDa dextrans and mycobacterial signals at each optical plane containing the two signals (Fig. 2*F*). The intensity of dextran fluorescence approached saturation at regions of colocalization, indicating complete access of the dextrans to the BCG phagosome (Fig. 2*E*). Despite signal colocalization in some optical planes within the series, however, occasionally a single optical plane did not (Fig. 2*I*). These bacteria were therefore conservatively scored as being not colocalized, existing instead within membrane-impermeable vacuoles. It was consistently found that only a proportion of the bacteria within a given infected cell was within membrane-permeable vesicles (Fig. 2*F*).

Access to the BCG-GFP Phagosome Is Size-Restricted. To address the limitations on membrane permeability facilitated by mycobacteria, colocalization was determined for at least 100 bacilli in each group, through successive optical sections, with a summary of the data presented in Fig. 3. Data collection was carried out immediately after verification of diffusion of the microinjected dye; however, examination of a large number of injected cells at least 10 minutes after microinjection revealed comparable phenomena. Tagged dextrans of 3 (35%) or 40 kDa (30%) in size and tagged ovalbumin (45 kDa) (26%) gained access to vesicles containing live BCG in >100 bacilli enumerated. Dextrans as large as 70 kDa accessed the BCG phagosome (14%); however, 2,000-kDa dextrans were effectively unable to access the BCG phagosome (3%). Thus, the size limit on the permeability of macromolecules induced by BCG infection appeared to be between 70 kDa and 2,000 kDa.

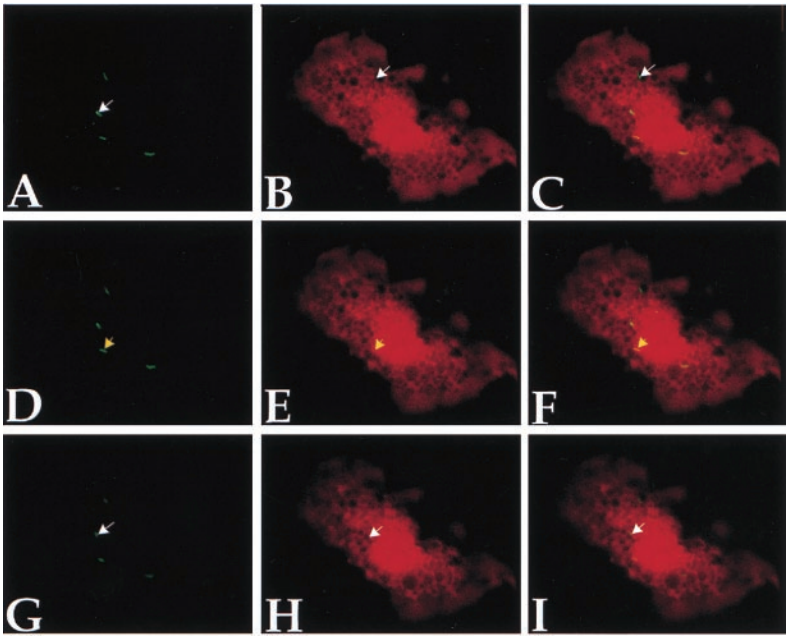

Fig. 2. Signal colocalization is not a plane of section artifact. BCG-GFP-infected macrophages were microinjected with 40-kDa-sized Texas Red-tagged dextrans and immediately were visualized by confocal microscopy. Successive optical sections were collected along the *z* axis, with a step of 0.9 μm. Three optical planes taken from the substratum up—*A–C*, *D–F*, and *G–I*—are shown. *A*, *D*, and *G* show fluorescence in the green channel only, *B*, *E*, and *H* show fluorescence in the red channel only, and *C*, *F*, and *I* are merged for RGB color. Numerous bacilli (*A*, white arrow) remained within clearly discernable vesicles impenetrable to the dextrans (*B*, white arrow), thereby precluding signal colocalization. Occasionally, yellow bacilli seemingly within compartments accessible to the dye appeared within an impermeable vesicle only after evaluation of several successive optical sections (compare bacteria in *I*, white arrow, with *C*). A significant number of BCG-GFP, however, facilitated dextran signal colocalization at every plane of section (*D–F*, yellow arrows).

Bacterial Strains Expressing a Membrane Lysin Access Cytoplasmic Macromolecules, Irrespective of Size. To determine whether bacterial strains known to exist within the host cell cytoplasm reveal a similar colocalization phenotype, GFP was introduced into an *L. monocytogenes* wild-type strain, as well as an hly chromosomal deletion mutant. hly encodes the pore-forming hemolysin listeriolysin O (LLO), that mediates the escape of *L. monocytogenes* from host cell vacuoles. *L. monocytogenes* strains lacking this gene product are known to be essentially avirulent (18). Wild-type *L. monocytogenes* strains expressing GFP (LLO + GFP), as expected, readily colocalized with injected dextrans as large as 2,000 kDa in size (Fig. 4 *A–C*), indicating free access of *L. monocytogenes* to cytosolic materials. hly deletion strains expressing GFP (LLO$^-$ + GFP), however, failed to exhibit signal colocalization with even the smallest sized (3 kDa) dextran, indicating a lack of vesicular membrane permeability (Fig. 4 *D–F*). Thus, listeria strains exiting the phagosome completely access cytosolic material whereas avirulent strains devoid of the lysin are contained within membrane impermeable vesicles.

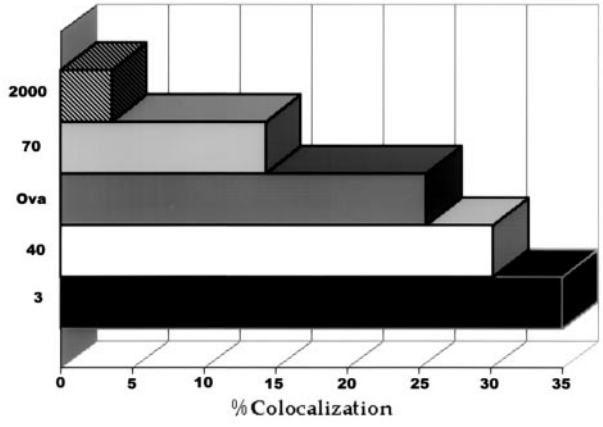

Fig. 3. BCG reside within vesicles permeable to cytosolic macromolecules of up to 70 kDa in size. Macrophages infected with BCG-GFP and microinjected with 3- or 40-kDa Texas Red-tagged dextrans or tagged-ovalbumin showed appreciable colocalization of the two signals. Microinjection of 70-kDa tagged dextrans into macrophages infected with live BCG-GFP demonstrates reduced colocalization, probably indicating an upper limit of accessibility to the phagosome. Injection of 2,000 kDa failed to reveal any appreciable signal colocalization.

Only Viable Mycobacterial Species of the *M. tuberculosis* Group Reside Within Membrane-Permeable Vesicles. To determine whether killed or other mycobacterial species could access the cytoplasm, macro-

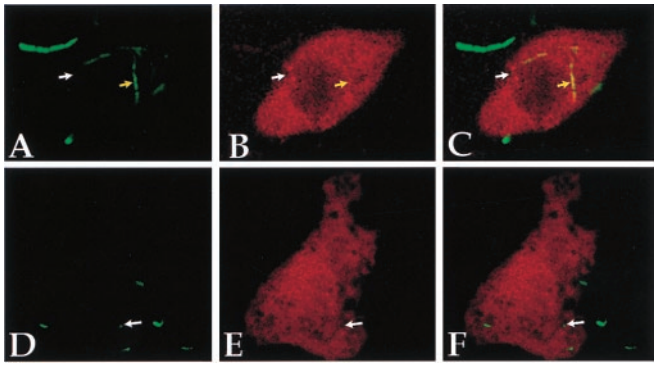

Fig. 4. Listeria strains expressing the listeriolysin O reveal colocalization with 2,000-kDa-sized macromolecules. Macrophages were infected with LLO$^+$-GFP (*A–C*) for 3 hours before microinjection with 2,000-kDa Texas Red-tagged dextrans and were visualized by confocal microscopy. LLO$^+$-GFP (*A*, yellow arrow) were readily observed within regions completely accessible to the large dextran molecules (*B*), thereby enabling colocalization of the two fluorescent signals (*C*). Macrophages infected with LLO-GFP (*D*, white arrow) then microinjected with 3-kDa Texas Red-tagged dextrans (*E*) failed to reveal signal colocalization (*F*).

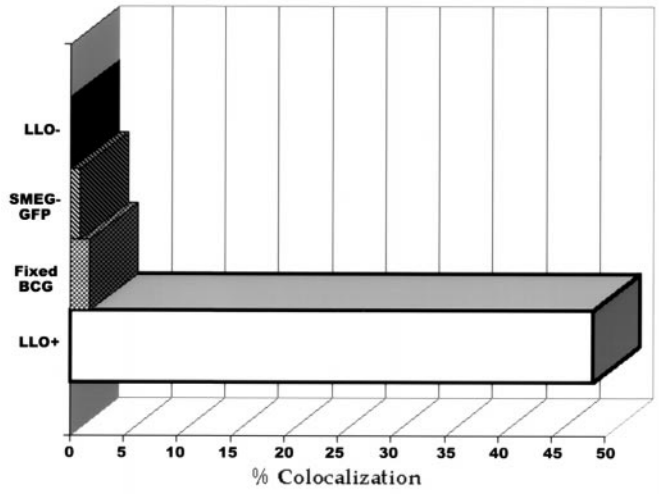

Fig. 5. Only viable mycobacterial strains of the tuberculosis complex, as well as listeriolysin O expressing *L. monocytogenes* strains, efficiently access the cytoplasm. Macrophages infected with killed BCG-GFP and microinjected with 3 kDa revealed no appreciable colocalization of the two signals, and neither did macrophages infected with live SMEG-GFP injected with 3- or 40-kDa-sized tagged dextrans. Intracytoplasmic microinjection of 3-kDa tagged dextrans in macrophages infected with LLO-GFP similarly demonstrate negligible colocalization, indicating bacterial residence within a membrane-impermeable vesicle. Injection of 2,000-kDa Texas Red-tagged dextrans in LLO+GFP revealed substantial signal colocalization (50%), indicating free access of the bacteria to cytoplamically located macromolecules.

phages were similarly infected with either formalin-killed BCG-GFP or a nonpathogenic species, *M. smegmatis* expressing GFP (SMEG-GFP). Infected macrophages were microinjected with tagged dextrans, and colocalization of signal was determined, as above. Quantitation of >100 bacilli of either formalin-killed BCG-GFP or SMEG-GFP failed to reveal colocalization of signal with even the smallest sized dextran (3 kDa), at any optical plane of section (2 and 1%, respectively) (Fig. 5). Examination of at least 50 bacilli at every plane of section revealed that 50% of LLO+ *L. monocytogenes* strains exhibited signal colocalization with molecules as large as 2,000 kDa. In contrast, LLO^- + GFP did not colocalize with 3-kDa-sized dextrans at any plane of section (0%). Thus BCG, like LLO-expressing *L. monocytogenes*, appear to have one or more molecules that allow access to cytoplasmic material, and that molecule appears only in viable organisms. Unlike LLO^+ strains, however, that putative molecule does not appear to liberate BCG from its vesicle, but instead allows a size-restricted access to cytosolic constituents.

Discussion

The study of microbial pathogenicity has revealed diverse intricate relationships between pathogens and cells of their mammalian hosts (19, 20). Some organisms grow extracellularly, others intracellularly in vacuoles, and others escape from vacuoles into the cytoplasm. The mechanisms by which pathogenic mycobacteria cause tissue damage and disease remain almost entirely unclear, even to the extent to which pathology is caused by products of the pathogen or the host immune response. There has, therefore, been much interest in the interactions of pathogenic mycobacteria and macrophages, the principal cells of the body in which they replicate. Escape of *M. tuberculosis* from its vacuole within infected macrophages has been reported by a number of investigators (21–24). Yet controversy remains as to whether these observations were artifact because of the experimental technique used (25, 26) or the use of an *in vitro* system (27). Although complete bacterial escape into the cytoplasm is one mechanism whereby an intracellular pathogen can provide protein access to the cytoplasm, the present data also support an alternative hypothesis of bacterial-mediated pore formation within the phagosomal membrane. The existence of a pore within the parasitophorous vacuole has been demonstrated for toxoplasma (28) and plasmodium (29).

There has been no resolution to date, however, as to how mycobacteria facilitate antigen presentation through the MHC class I pathway. Studies revealed that β_2M-deficient mice, deficient in the ability to present antigen through the MHC class I pathway, are more susceptible to *M. tb* or BCG infection, implicating a role for CD8 cytotoxic T lymphocytes in controlling *M. tb* infection (2, 30). *In vitro* evidence has revealed that MHC class I-restricted T cells can exert cytotoxicity *in vitro* against infected target cells (31, 32). Human CD8 T cells have been found to kill *M. tb* infected macrophages *in vitro* and reduce the viability of intracellular bacteria (33), and, thus, mechanisms governing this phenomenon may have therapeutic value.

Because of the limitations of resolving the question of intracellular trafficking by electron microscopic analysis, we previously developed functional evidence that *M. tb* and BCG can facilitate antigen presentation *in vitro* to T cells through a TAP-dependent MHC class I-restricted pathway (6). Although *M. tb* infection of macrophages allowed soluble antigens to be presented to MHC class I-restricted T cells, the mechanism by which a vacuolar membrane-bound organism can gain access to the host cell cytoplasm remained undefined. Whether intact antigens enter the cytoplasm to be degraded by the proteasome machinery or whether only small peptides derived from the cleavage of antigens within the phagosome access the host cell cytoplasm are questions it has not been possible to address by the model systems previously used.

The present experiments were undertaken to define the limit, if any, of accessibility to the mycobacterial phagosome. Using a dynamic system of real time observation of living cells offered by confocal microscopy, we found that BCG infection of macrophages created access of cytoplasmic macromolecules to the bacillus-containing vacuole. At a time optimal for MHC class I presentation of soluble antigen to T cells, cytoplasmically located markers readily accessed the phagosome. Although peptides may exit the phagosome and enter the cytosol for antigen presentation, intact protein and macromolecules of between 40 and 70 kDa were found to have the capacity to enter, and presumably to exit, the phagosome of BCG-infected macrophages.

Only live BCG organisms were able to create phagosomal membrane permeability; formalin-fixed bacilli precluded even 3-kDa-sized molecule entry within the mycobacterial phagosomes. Although studies with LLO^+ and LLO^- listeria revealed that the LLO^+ bacteria, known to escape their phagocytic vacuoles and enter the cytoplasm rapidly, colocalized with 2,000-kDa dextrans, LLO^--containing vesicles were completely impenetrable. Yet studies with BCG revealed a size-restricted limit to the colocalization of the tagged cytoplasmic marker molecules of between 3 and 70 kDa, indicating that BCG were almost certainly retained within membrane-bound vesicles and were not completely free in the cytoplasm. Although 70-kDa-sized molecules were able to access the phagosome, the percent colocalization of the two signals was somewhat diminished, probably indicating the upper limit of access to the phagosome. In our studies, as in the studies demonstrating presentation of soluble antigen to cytotoxic T lymphocytes through MHC class I, only viable bacteria were able to do so. Formalin-fixed BCG, live *M. smegmatis*, or listeriolysin O-deficient *L. monocytogenes* failed to present antigen through the MHC class I pathway, as described (6), or colocalize with the cytoplasmic marker. It is thus apparent that some mycobacterial species residing within membrane permeable phagosomes can access cytoplasmically located host factors; moreover, other organisms accessing the host cell cytoplasm, known to completely exit the phagosome, such as listerial strains expressing the listeriolysin O, reveal no size-

restricted access to the cytoplasm. The data indicated that BCG, in contrast to listeria, uniquely accesses macromolecules within a specific size-range while concurrently providing access of mycobacterial antigens to the MHC class I antigen presentation pathway. These data are most consistent with a model in which viable mycobacteria may release molecules that create pores in the vesicular membrane.

It is attractive to speculate that a pore within the phagosomal membrane could facilitate bi-directional transport of nutrients to, and antigens from, the mycobacterial phagosome, similar to what has been shown for *Toxoplasma gondii*, using a similar experimental system (28). The biosynthesis and possible secretion of a pore-forming molecule by BCG and *M. tb* would explain the finding of a molecular size-restricted entry within the phagosome, without complete escape from a membrane vacuole. It is possible, however, that a dissolving membrane might show a similar size restriction, and that at some point some organisms might have full access to cytoplasmic macromolecules of all sizes. Our functional *in vitro* results are fully consistent with both previous functional (6) and electron microscopic results (3, 23) with *M. tuberculosis*. Previous comparative data on the relative abilities of *M. tb* and BCG to allow MHC class I presentation indicated that *M. tb* was severalfold more effective in providing access of soluble antigens from the vacuole to the cytoplasm. We believe the present results would be even stronger had we been able to carry out comparable experiments using virulent *M. tb*.

Some investigators have criticized the use of conventional microscopic techniques to determine the state of the phagosomal membrane in *M. tb* infected macrophages (25). We believe that our demonstration of membrane permeability obviates artifacts in transmission electron microscopy such as a fixation or processing distortion because we used a live-cell, real time system. Furthermore, we considered the possibility that the limit of resolution of the light microscope might be responsible for apparent colocalization of the indicator signal and BCG, but believe it to be highly unlikely. Numerous controls used in these studies, including killed BCG, live *M. smegmatis*, and listeria deficient in the listeriolysin O protein, as well as the majority of live bacilli examined within each size range, failed to demonstrate signal colocalization. Should signal colocalization be a result of the limit of resolution of the microscope along the *x* and *y* axes, signal colocalization would be expected to occur in each of these controls as well, which was clearly not the case. It could be argued that the apparent colocalization of the signals is attributable to diminished resolution along the *z* axis. Although a step of 0.9 μm was used, and the bacilli are <0.5 μm in diameter, colocalization was only scored if every plane of section in an optical series revealed signal colocalization. Because mycobacteria are ≈ 4 μm in length, our results are therefore not attributable to a limit of resolution artifact. Similarly, we imaged 0.5-μm Oregon green-tagged beads suspended in Texas Red-tagged 3-kDa dextrans. Upon viewing every plane of optical section, these beads were readily resolved as excluding the Texas Red-tagged dextrans, indicating that the resolution in the *z* axis was sufficient. Finally, we can exclude the possibility that colocalization was a result of cellular autophagy of the indicator dye within vacuoles containing BCG. Data collection immediately followed microinjection in these studies, such that typically <3 seconds elapsed from the time of injection to the time of the initiation of z series collection, an insufficient period of time to enable autophagy to occur. Imaging of these cells at 10 minutes after microinjection revealed the same phenomenon.

It is our conclusion that BCG, and almost certainly *M. tb*, after uptake by macrophages do not remain within membrane-limiting vacuoles. Permeabilization of the vacuolar membrane may enable the bacilli to obtain key nutrients available in the host cell cytoplasm, not otherwise available to bacilli within an impermeable vacuole. An alternative benefit of mycobacterial access to the cytoplasm may be the ability to direct toxic mycobacterial products, such as cord factor, to the host cell cytoplasm. In this manner, toxic products may exert their effects directly on cytoplasmically located organelles, such as mitochondria, shown to be sensitive to mycobacterial products *in vitro* (34). The consequence of this exposure may be host cell and ultimately tissue death, a prominent characteristic of tuberculosis infection *in vivo*, which may be essential for the transmission of the pathogen via the respiratory route between individuals. Although mycobacterial pathogenesis may be furthered by the permeabilization of the phagosome, it concurrently enables the establishment of an immune response shown to be effective in reducing mycobacterial viability (33, 2). Thus, the study of the interaction of bacterium and macrophage continues to reveal how complex, dynamic, and subtle are the interactions between mycobacteria and cells of their hosts.

This work was supported by National Institutes of Health Grants AI07118 and AI23545 and the Howard Hughes Medical Institute.

1. Orme, I. M. & Collins, F. M. (1984) *Cell. Immunol.* **84,** 113–120.
2. Flynn, J. L., Goldstein, M. M., Triebold, K. J., Koller, B. & Bloom, B. R. (1992) *Proc. Natl. Acad. Sci. USA* **89,** 12013–12017.
3. Clemens, D. L. & Horwitz, M. A. (1996) *J. Exp. Med.* **184,** 1349–1355.
4. Hasan, Z., Schlax, C., Kuhn, L., Lefkovits, I., Young, D., Thole, J. & Pieters, J. (1997) *Mol. Microbiol.* **24,** 545–553.
5. Germain, R. N. & Margulies, D. H. (1993) *Annu. Rev. Immunol.* **11,** 403–450.
6. Mazzaccaro, R. J., Gedde, M., Jensen, E. R., van Santen, H. M., Ploegh, H. L., Rock, K. L. & Bloom, B. R. (1997) *Proc. Natl. Acad. Sci. USA* **93,** 11786–11791.
7. Kovacsovics-Bankowski, M. & Rock, K. L. (1995) *Science* **267,** 243–246.
8. Cormack, B. P., Valdivia, R. H. & Falkow, S. (1996) *Gene* **173,** 33–38.
9. Stover, C. K., de la Cruz, V. F., Fuerst, T. R., Burlein, J. E., Benson, L. A., Bennett, L. T., Bansal, G. P., Young, J. F., Lee, M. H., Hatfull, G. F. *et al.* (1991) *Nature (London)* **351,** 456–460.
10. Wards, B. J. & Collins, D. M. (1996) *FEMS Microbiol. Lett.* **145,** 101–105.
11. Jacobs, W. R., Jr., Kalpana, G. V., Cirillo, J. D., Pascopella, L., Snapper, S. B., Udani, R. A., Jones, W., Barletta, R. G. & Bloom, B. R. (1991) *Methods Enzymol.* **204,** 537–555.
12. Freitag, N. E., Rong, L. & Portnoy, D. A. (1993) *Infect. Immun.* **61,** 2537–2544.
13. Jones, S. & Portnoy, D. A. (1994) *Infect. Immun.* **62,** 5608–5613.
14. Yansura, D. G. & Henner, D. J. (1984) *Proc. Natl. Acad. Sci. USA* **81,** 439–443.
15. Denoya, C. D., Bechhofer, D. H. & Dubnau, D. (1986) *J. Bacteriol.* **168,** 1133–1141.
16. Park, S. F. & Stewart, G. S. A. B. (1990) *Gene* **94,** 129–132.
17. Pawley, J. (1989) in *Handbook of Biological Confocal Microscopy*, ed. Pawley, J. (Plenum, New York), pp. 19–37.
18. Portnoy, D. A., Chakraborty, T., Goebel, W. & Cossart, P. (1992) *Infect. Immun.* **60,** 1263–1267.
19. Finlay, B. B. & Cossart, P. (1997a) *Science* **276,** 718–725.
20. Finlay, B. B. & Falkow S. (1997b) *Microbiol. Mol. Biol. Rev.* **61,** 136–169.
21. Armstrong, J. A. & Hart, P. D. (1975) *J. Exp. Med.* **142,** 1–16.
22. Kondo, E., Yasuda, T. & Kanai, K. (1982) *Jpn. J. Med. Sci. Biol.* **35,** 197–201.
23. McDonough, K. A., Kress, Y. & Bloom, B. R. (1993) *Infect. Immun.* **61,** 2763–2773.
24. Myrvik, Q. N., Leake, E. S. & Wright, M. J. (1984) *Am. Rev. Respir. Dis.* **129,** 322–328.
25. Clemens, D. L. & Horowitz, M. A. (1995) *J. Exp. Med.* **175,** 257–270.
26. Clemens, D. L. (1996) *Trends Microbiol.* **4,** 113–118.
27. Moreira, A. L., Wang, J., Tsenova-Berkova, L., Hellmann, W., Freedman, V. H. & Kaplan, G. (1997) *Infect. Immun.* **65,** 305–308.
28. Schwab, J. C., Beckers, C. J. & Joiner, K. A. (1994) *Proc. Natl. Acad. Sci. USA* **91,** 509–513.
29. Desai, S. A., Krogstad, D. J. & McCleskey, E. W. (1993) *Nature (London)* **362,** 643–646.
30. Ladel, C. H., Daugelat, S. & Kaufmann, S. H. (1995) *Eur. J. Immunol.* **25,** 377–384.
31. De Libero, G., Flesch, I. & Kaufmann, S. H. (1988) *Eur. J. Immunol.* **18,** 59–66.
32. Bonato, V. L., Lima, V. M., Tascon, R. E., Lowrie, D. B. & Silva, C. L. (1998) *Inf. Immun.* **66,** 169–175.
33. Stenger, S., Mazzaccaro, R. J., Uyemura, K., Cho, S., Barnes, P. F., Rosat, J. P., Sette, A., Brenner, M. B., Porcelli, S. A., Bloom, B. R. & Modlin, R. L. (1997) *Science* **276,** 1684–1687.
34. Kato, M. (1969) *Am. Rev. Respir. Dis.* **100,** 47–53.